Chem Rep, 2019, 1(2): 51-57
DOI: 10.25082/CR.2019.02.001

RESEARCH ARTICLE

Azo-dye adsorption activity of iron(III) loaded novolac-based network sorbents

Samaresh Ghosh[1*] Mridula Acharyya[1]

Abstract: Iron(III) loaded novolac-based network adsorbents 1 and 2 were studied for efficient removal of azo-dye pollutants from aqueous solutions. The adsorption behavior was evaluated by using methyl orange and orange-G as model azo dyes. The effect of parameters such as contact time and initial dye concentration on the adsorption of azo dyes was studied. The results showed that loading of Fe(III) onto the sorbent networks has noticeable effect on azo-dye sorption capacity. The adsorption equilibrium data were fitted to Freundlich isotherm model. Besides, the reusability of the dye loaded sorbents was investigated on adjusting pH of solutions.

Keywords: adsorption, novolac-based network, iron(III) loading, azo-dye

1 Introduction

With the fast growth in the usage of azo-dye colorants in many dyestuffs and allied industries, azo-dye pollution in water stream has become a major environmental problem. Some of the azo dyes originating from the effluents of industrial sites and their degradation products are connected to toxic, carcinogenic and mutagenic effects on human health and marine organisms.[1–5] Therefore, there is an urgent need to treat effluents before dischange into water bodies. Various physico-chemical methods including coagulation and flocculation, oxidation or ozonization, membrane-filtration processes, ion exchange, chemical precipitation, and adsorption focused on the removal of azo dyes from wastewater.[6–17] Among these methodologies, adsorption-based process[6–8] has received increasing interest because of its economics, design simplicity and efficiency in minimizing pollutants. Polymeric sorbents[18–36] enjoy exclusive attributes namely low density, high thermal and/or chemical stability, mechanical rigidity, wide variations in porosity and surface functionality tailoring, high adsorption capability, easy handling and feasible regeneration. Phenolic resins due to their low-cost, easy availability, and dimensional stability, are popular for innovative applications in various domains. These polymers by their structural features are particularly appealing in the design of new macromolecular sorbent materials for the removal of dye pollutants from waters. In this direction, our research group has paid attention on the design of novolac type phenolic resin-based network polymers for eliminating azo dye contaminants from water.[27,31] Adequate functionality in this network can allow interaction with metal ions constituting new type of hybrid materials. In the present work, we focused on the preparation of iron(III) loaded novolac-based networks **1** and **2** (Figure 1) to apply on the adsorptive removal of azo-dye pollutants from aqueous media.

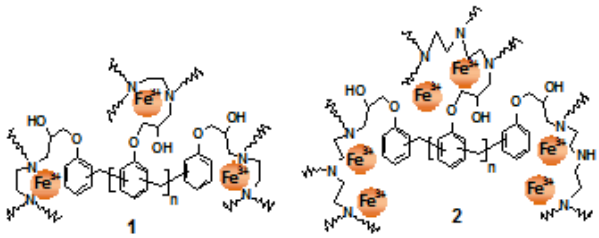

Figure 1. Iron(III) loaded novolac-based networks 1 and 2

2 Experimental

2.1 Preparation of adsorbents 1 and 2

Adsorbents **1** and **2** were prepared using $Fe(NO_3)_3$ and novolac-based precursor networks **1a** and **2a** as produced from our published method.[27,31] In a typical

Received: March 29, 2019 **Accepted:** April 17, 2019 **Published:** April 19, 2019

*Correspondence to: Samaresh Ghosh, Department of Chemistry, Bankura Sammilani College, Kenduadihi, Bankura 722102, West Bengal, India; Email: gsamaresh@yahoo.com

[1] Department of Chemistry, Bankura Sammilani College, Kenduadihi, Bankura 722102, West Bengal, India.

Citation: Ghosh S and Acharyya M. Azo-dye adsorption activity of iron(III) loaded novolac-based network sorbents. *Chem Rep*, 2019, **1**(2): 51-57.

preparation, network and iron(III) nitrate nonahydrate [$Fe(NO_3)_3.9H_2O$] were first mixed in the ratio (1:10, w/w) in deionised water and left for adsorption for 24 h. The network was then filtered, and impregnated with deionized water for another 24 h. The solid separated by filtration, washed thoroughly with deionized water and dried for 12 h at 50-60°C to yield Fe(III) loaded network. The filtrates and washings were combined. The amount of Fe(III) loaded onto the network was evaluated by measuring the concentration of Fe^{3+} remaining in combined solution using UV-vis spectrophotometric method by measuring maximum absorbance of ferric thiocyanate color complex, located at λ = 480 nm. Graphical plot of absorbance (y axis) against Fe^{3+} (aq) concentration was used to find the concentration of Fe^{3+} in aqueous solution after adsorption. Iron content in **1** and **2** were estimated to be 38 mg/g and 85 mg/g respectively.

2.2 Adsorption experiments

The batch adsorption experiments were conducted by adding pre-weighed amount of sorbents to the aqueous solution of azo dye at pH 7.20 and shaken at room temperature. The pH was adjusted to a given value with dilute NaOH or HCl solutions. The solutions were periodically separated from the adsorbents, and the residual concentrations of azo dyes were estimated by UV-vis spectrophotometer at λ_{max} = 484 nm. The amount of dye adsorbed (mg/g) at equilibrium was calculated by using the formula: $q_e = [(C_0 - C_e)\,V]\,/W$; where C_0 and C_e are the initial and equilibrium dye concentrations (mg/L) respectively. V is the volume of solution (L), W is the weight of the sample (g). Freundlich isotherm model was employed to assess the adsorption equilibrum. The logarithmic form of the Freundlich equation is represented by the following equation: $\ln q_e = \ln K_f + 1/n \ln C_e$ where K_f and n are Freundlich constants related to the adsorption capacity and adsorption intensity, respectively. K_f and 1/n were obtained from the linear plot of ln q_e *vs.* ln C_e.

2.3 Desorption and regeneration experiments

Azo-dye loaded adsorbents were kept in deionised water and the pH of the medium was adjusted to 12.0 by adding dilute NaOH solution. The mixtures were shaken at 25°C for a period of 24h to desorb azo dyes (MO/OG). Thereafter, the regeneration process of adsorbents was performed by putting them in fresh deionised water. The pH was adjusted to neutral with dilute HCl. The resulting regenerated sorbents were filtered, dried and reused in the next cycle. The adsorption/desorption process was repeated three times.

3 Results and discussion

3.1 Synthesis and characterization

Recently, polymer/inorganic hybrid materials have attracted interest to remove trace pollutants from waters.[24,30] Their unique properties arise from the combination of both polymer and inorganic characteristics. Novolac-based network polymers **1a** and **2a** deserve particular attention in loading metal ions especially ferric minerals, due to the nonhydrolyzable polyfunctionality in combination with the feature of novolac structural support providing mechanical, chemical, and thermal strength. The ligating groups (amino, hydroxyl) in their backbone have the ability to complex with Fe(III). This might avoid dissolution of Fe(III) in the medium during waste treatment applications. Figure 2 illustrates the loading of Fe(III) ions in the networks to yield **1** and **2**.

Iron(III) loaded networks **1** and **2** were characterized by FTIR and XRD analyses. FTIR spectra of **1** and **2** show the broad band located in the region 3000 − 3500 cm^{-1}, assignable to the O-H and N-H stretching frequencies Compared to **1a** and **2a**, this band was found to be further broadened and shited to longer wavenumbers ($\Delta\nu$ = 25-30 cm^{-1}) indicating the involvement of ferric ions in coordination with amino and hydroxyl moieties in association with the coordinated water molecules. Furthermore, there were shifts to longer wavenumbers ($\Delta\nu$ = 6-27 cm^{-1}) of O–H bending vibrations appearing at 1610 cm^{-1} and 1627 cm^{-1} when iron loaded onto the networks. The shifting of these peaks to longer values underlines the presence of coordinated OH groups in the networks. The absorption band near 1382 cm^{-1} appeared due to the vibrations of nitrate ions,[37,38] which confirms the incorporation of ferric nitrate in the networks. Figure 3 shows the XRD pattern of **2**. The pattern showing broad peak centered at 2θ = 21.22^0 and very low intensity peak centered at 2θ = 40.75^0 was characteristic for amorphous material. The appearance of no sharp peaks further indicates the amorphous structure of Fe^{3+} salt loaded within the polymer matrix. This could be advantageous since amorphous compounds are known to be especially effective in achieving adsorption compared to crystalline forms.[39]

3.2 Adsorption evaluation

Molecular structures of methyl orange (MO) and orange-G (OG) employed in the evaluation of adsorption abilities of **1** and **2** are shown in Figure 3. The absorption spectra of both MO and OG in water exhibit characteristic absorption band peaked at 484 nm (Figure 4).

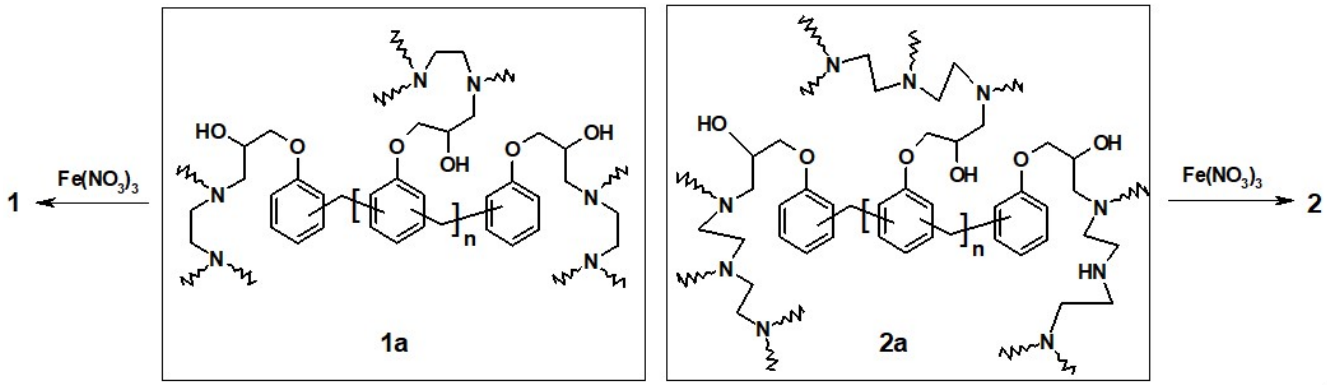

Figure 2. Preparative scheme for iron(III) loaded novolac-based sorbents **1** and **2**

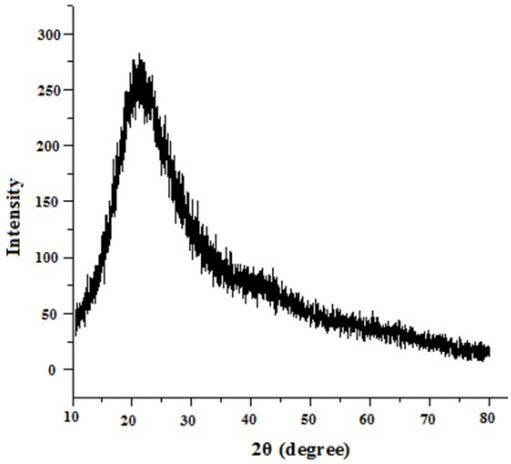

Figure 3. The XRD pattern of **2**

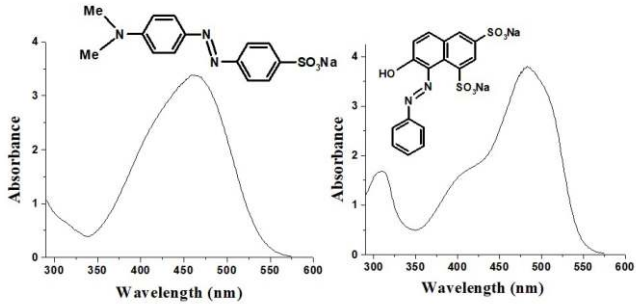

Figure 4. Molecular structures and UV-vis spectra of azo dyes: (a) Methylorange: 7.64 × 10^{-5}M and (b) Orange-G: 2.21 × 10^{-4}M

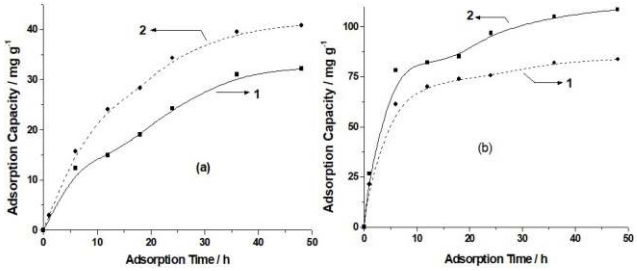

Figure 5. The effect of adsorption time on azo-dye adsorption of **1** and **2** at pH = 7.20 (a) MO adsorption (C_0 = 50 mg/L; 1.52 × 10^{-4}M); (b) OG adsorption (C0 = 150 mg/L; 3.31 × 10^{-4}M)

We examined azo dye adsorption behaviors as a function of contact time at pH 7.20. Adsorbents **1** and **2** exhibit significant dye removal bebavior for MO and OG as estimated from the decrease in maximum absorbance at 484 nm. As shown in Figure 5, the rapid adsorption at the initial stage was occurred and reached a nearly equilibrium within 48 h. This could probably be attributed to the abundance of unoccupied adsorption sites. The dye adsorption gradually slowed down with time which is probably associated with the slow diffusion of the dye molecules into the sorbents porous structures. The rapid adsorption at the initial stage demonstrates the suitability of the sorbents in reducing reactor volumes and times.

Figure 6 displays the effect of Fe(III) loading on the adsorptive removal of MO and OG. Network **2** has higher dye uptake capacity compared to **1** due to higher loading of Fe(III). The results of azo-dye removal by **1a** and **2a** have recently been reported by our group.[31] However, under comparable conditions **1** and **2** achieved higher adsorption capacities than **1a** and **2a** which was attributed to the role of Fe(III) being immobilized onto the networks. In addition, sorbents **1** and **2** showed higher uptake of OG than MO indicating more favorable interaction.

The visual changes in color of the azo dye solutions from red to very light yellow during the same process were recorded in Figure 7. This result demonstrates the effective adsorptive response of sorbents in color removal.

Meanwhile, the adsorbents **1** and **2** turned to deep red and orange after adsorbing MO and OG, respectively (Figure 8). This accounted for a visual indication of MO/OG loaded sorbent surfaces.

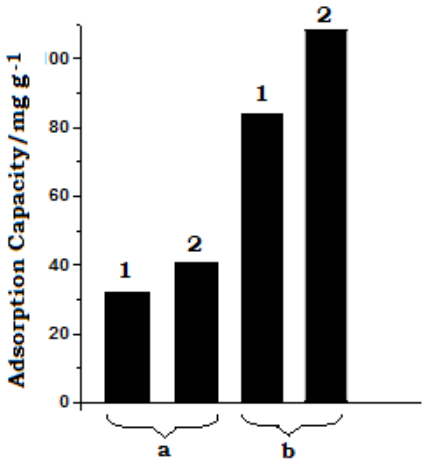

Figure 6. Azo dye adsorption capacity of **1** and **2** (pH = 7.20; t = 48h; T= 298 K); (a) MO adsorption (C_0 = 50 mg L^{-1}; 1.52 x 10^{-4}M); (b) OG adsorption (C_0 = 150 mg L^{-1}; 3.31 x 10^{-4}M)

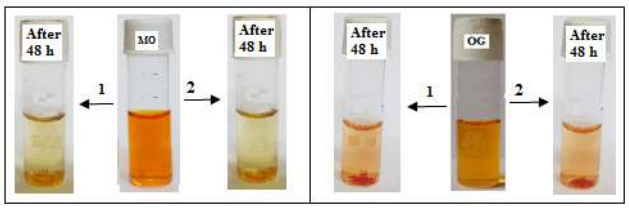

Figure 7. Color changes of MO and OG solutions before and 48 h after adsorption onto **1** and **2** at pH = 7.20

Freundlich model[40,41] was used to fit the equilibrium adsorption isotherm data. The model parameters along with the correlation coefficients (R^2) were listed in Table 1. The K_f values revealed the good adsorption capacity of both **1** and **2**. The value of n in the range 1-10 indicated thermodynamically favorable adsorption. The values of R^2 reflected adequate description of dye adsorption by Freundlich isothermal model. Therefore, iron loading in the networks provides new kind of materials applicable in the manipulation of azo dye adsorption capacities.

Table 1. Freundlich fitting parameters in MO and OG adsorption isotherms for the studied samples at pH 7.20

Fe(III) loaded polymer network	Azodye	Freundlich Constants		
		K_f	n	R^2
1	MO	2.027	1.044	0.9729
	OG	39.251	4.594	0.9731
2	MO	9.55	1.448	0.9971
	OG	41.952	3.855	0.9868

To further explore the reusability, the adsorption-desorption cycle was repeated upon pH adjustment with

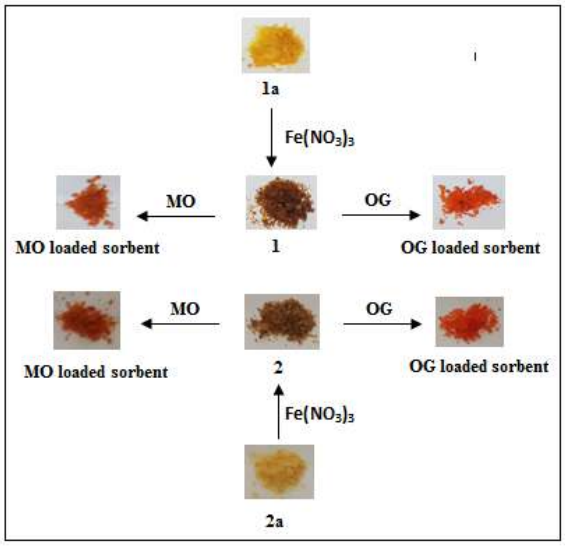

Figure 8. Photographs of sorbents on adsorption of MO and OG after 48h

dilute HCl or NaOH solutions. As presented in Figure 9, the desorptions are visually followed by gradual disappearance of sorbents colors, and the color development in aqueous solutions. We found that more than 90% desorption happens during 24 h in the alkaline condition (pH $\approx$ 12.0). UV-vis spectral investigation quantified the desorbed amount of azo dyes (MO/OG). After desorption the sorbents were regenerated by pH adjustment to 7.0 and reused for a number of cycles for its adsorption efficacy. However, adsorption efficiency remained comparable with increasing cycle number. After three consecutive cycles, the azo dye adsorption efficiency is still above 80%. This is quite important not only in the effective regeneration and reuse of the sorbents, but also the reuse of recovered azo dyes during the dyeing process impacting associated environmental issue.

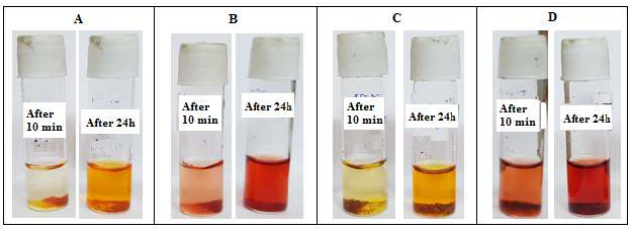

Figure 9. Desorption of MO and OG from dye loaded networks in water at pH = 12.0 (A) MO loaded **1** (B) OG loaded **1**(C) MO loaded **2** and (D) OG loaded **2**

The qualitative information on the chemical interactions was obtained from the FTIR spectral analysis of the dye-adsorbed networks (dry). The broad absorption band in the region 3200-3500 cm^{-1} (O-H and N-H stretching) experienced better resolution when dye

adsorbed. In addition, the stretching vibrations of azo-dye SO_3^- groups shifted to lower wavenumber ($\Delta\nu$= 2-9 cm^{-1}) appearing at 1171 and 1033 cm^{-1} with reduced intensity when loaded onto the sorbents. This is ascribed to the interaction of sorbents with azo dyes through SO_3^- groups. The decrease in intensity of the NO_3^- peak (1382 cm^{-1}) also occurred, which indicated ion exchange sorption of anionic azo dye molecules. On the basis of our previous reports[27,31] and experimental observations, the proposed mechanism for dye adsorption and desorption is outlined in Figure 10. In this context, structures of MO and OG and iron species loaded onto the network having a variety of interacting motifs (amino, hydroxy and ether functionalities) must be taken into account. Iron species might create more active sites synergic with functional adsorptive motifs of networks to cater more azo dye pollutants on the surface. The involvement of physical forces, such as metal ion coordination as well as hydrogen bonding interactions involving functional groups of dye molecules (Fe^{3+} —— ^-O_3S-Dye, and Network–O-H —— ^-O_3S-etc) might account for higher adsorption capacity (Figure 7, Figure 8). It is worth to note the occurrence of desorption of azo dyes from sorbents in the very basic condition (pH ≈12.0). This likely is related to the change of Fe^{3+} to $Fe(OH)_3$ and other complex hydroxides embedded in the network, which make the materials redundant favoring desorption. In addition, desorption might be related to the high enough concentration of hydroxyl ions (OH^-) competing with the anionic dye molecules (Dye-SO_{3^-}) for adsorption sites.

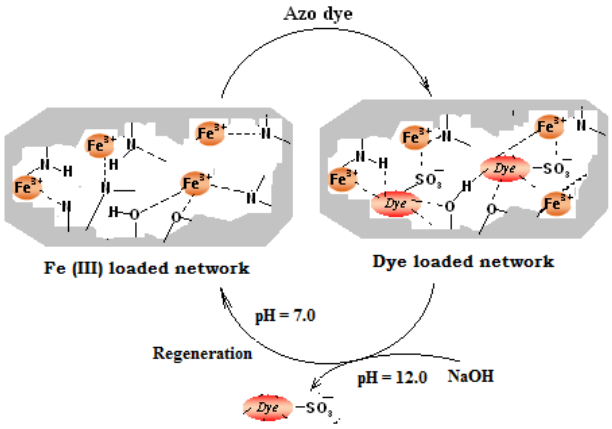

Figure 10. A proposed mechanism of adsorption-desorption of azo dye pollutants onto the sorbent networks

4 Conclusion

Iron(III) loading onto the novolac-based networks facilitates enhanced adsorption capacity for azo dye molecules. Adsorbent **2** with more iron(III) loading shows high adsorption capacities toward azo dye pollutants (MO and OG). Equilibrium adsorption phenomenon was expressed using Freundlich isotherm. The result indicates that adsorption is a typical physical process (n>1). The feasible mechanism toward azo-dye removal was proposed. Quite effective adsorption-desorption-regeneration-reuse cycle under pH adjustment offers great economic potential for sustainable remediation of azo-dye containing wastewaters. Further study is under progress in our laboratory.

5 Conflicts of Interest

No potential conflict of interest was reported by the authors.

References

[1] Chung KT. Mutagenicity and carcinogenicity of aromatic amines metabolically produced from azo dyes. Journal of Environmental Science and Health, Part C, 2000, **18**: 51-74. https://doi.org/10.1080/10590500009373515

[2] Chung KT. Azo dyes and human health: A review. Journal of Environmental Science and Health, Part C: Environmental Carcinogenesis Reviews, 2016, **34**: 233-261. https://doi.org/10.1080/10590501.2016.1236602

[3] Golka K, Kopps S and Myslak ZW. Carcinogenicity of Azo Colorants: Influence of Solubility and Bioavailability-A Review. Toxicology Letters, 2004, **151**: 203-210. https://doi.org/10.1016/j.toxlet.2003.11.016

[4] Tsuboy MS, Angeli JPF, Mantovani MS, *et al*. Genotoxic, mutagenic and cytotoxic effects of the commercial dye CI Disperse Blue 291 in the human hepatic cell line HepG2. Toxicologie Cellulaire in Vitro, 2007, **21**: 1650-1655. https://doi.org/10.1016/j.tiv.2007.06.020

[5] Brüschweiler BJ and Merlot C. Azo dyes in clothing textiles can be cleaved into a series of mutagenic aromatic amines which are not regulated yet. Regulatory Toxicology and Pharmacology, 2017, **88**: 214-226. https://doi.org/10.1016/j.yrtph.2017.06.012

[6] Sun SP, Li CJ, Sun JH, *et al*. Decolorization of an azo dye Orange G in aqueous solution by Fenton oxidation process: effect of system parameters and kinetic study. Journal of Hazardous Materials, 2009, **161**: 1052-1057. https://doi.org/10.1016/j.jhazmat.2008.04.080

[7] Ayati A, Ahmadpour A, Bamoharram FF, *et al*. Novel Au NPs/Preyssler acid/TiO_2 nanocomposite for the photocatalytic removal of azo dye. Separation and Purification Technology, 2014, **133**: 415-420. https://doi.org/10.1016/j.seppur.2014.06.055

[8] Zhang M, Yao Q, Lu C, *et al*. Layered Double Hydroxide-Carbon Dot Composite: High-Performance Adsorbent for Removal of Anionic Organic Dye. ACS Applied Materials & Interfaces, 2014, **6**: 20225-20233. https://doi.org/10.1021/am505765e

[9] Forgacs E, Cserhati T and Oros G. Removal of synthetic dyes from wastewaters: a review. Environment International, 2004, **30**: 953-971. https://doi.org/10.1016/j.envint.2004.02.001

[10] Rodriguez A, Ovejero G, Sotelo JL, *et al*. Heterogeneous Fenton Catalyst Supports Screening for Mono Azo Dye Degradation in Contaminated Wastewaters. Industrial & Engineering Chemistry Research, 2010, **49**: 498-505. https://doi.org/10.1021/ie901212m

[11] Ahmadi M, Ardakani MH and Zinatizadeh AA. Optimization and kinetic evaluation of acid blue 193 degradation by UV/peroxydisulfate oxidation using response surface methodology. Advances in Environment Technology, 2015, **2**: 59-68.

[12] Yao L, Zhang LZ, Wang R, *et al*. A new integrated approach for dye removal from wastewater by polyoxometalates functionalized membranes. Journal of hazardous materials, 2016, **301**: 462-470. https://doi.org/10.1016/j.jhazmat.2015.09.027

[13] Mines PD, Byun J, Hwang Y, *et al*. Nanoporous networks as effective stabilization matrices for nanoscale zero-valent iron and groundwater pollutant removal. Journal of Materials Chemistry A, 2016, **4**(2): 632-639. https://doi.org/10.1039/C5TA05025A

[14] Shana Z, Luc M, Curry DE, *et al*. Regenerative nanobots based on magnetic layered double hydroxide for azo dye removal and degradation. Chemical Communications, 2017, **53**: 10456-10458. https://doi.org/10.1039/C7CC05081J

[15] Mbarek WB, Azabou M, Pineda E, *et al*. Rapid degradation of azo-dye using Mn-Al powders produced by ball-milling. Rsc Advances, 2017, **7**: 12620-12628. https://doi.org/10.1039/C6RA28578C

[16] Bhatia D, Sharma NR, Singh J, *et al*. Biological methods for textile dye removal from wastewater: A review. Critical Reviews in Environmental Science and Technology, 2017, **4**7: 1836-1876. https://doi.org/10.1080/10643389.2017.1393263

[17] Rajabi M, Mahanpoor K and Moradi O. Removal of dye molecules from aqueous solution by carbon nanotubes and carbon nanotube functional groups: critical review. Rsc Advances, 2017, **7**: 47083-47090. https://doi.org/10.1039/C7RA09377B

[18] Geethakarthi A and Phanikumar BR. Industrial sludge based adsorbents/ industrial by-products in the removal of reactive dyes - A review. International Journal of Water Resources and Environmental Engineering, 2011, **3**: 1-9.

[19] Chen M, Ding W, Wang J, *et al*. Removal of Azo Dyes from Water by Combined Techniques of Adsorption, Desorption, and Electrolysis Based on a Supramolecular Sorbent. Industrial & Engineering Chemistry Research, 2013, **52**: 2403-2411. https://doi.org/10.1021/ie300916d

[20] Tomic NM, Dohcevic-Mitrovic ZD, Paunovic NM, *et al*. Nanocrystalline CeO2-δ as Effective Adsorbent of Azo Dyes. Langmuir, 2014, **30**: 11582-11590. https://doi.org/10.1021/la502969w

[21] Ayati A, Shahrak MN, Tanhaei B, *et al*. Emerging adsorptive removal of azo dye by metal-organic frameworks. Chemosphere, 2016, **160**: 30-44. https://doi.org/10.1016/j.chemosphere.2016.06.065

[22] Seow TW and Lim CK. Removal of dye by adsorption: A review. International Journal of Applied Engineering Research, 2016, **11**: 2675-2679.

[23] Chen F, Wu X, Bua R, *et al*. Co-Fe hydrotalcites for efficient removal of dye pollutants via synergistic adsorption and degradation. RSC Advances, 2017, **7**: 41945-41954. https://doi.org/10.1039/C7RA07417D

[24] Blachnio M, Budnyak TM, Marczewska AD, *et al*. Chitosan-Silica Hybrid Composites for Removal of Sulfonated Azo Dyes from Aqueous Solutions. Langmuir, 2018, **34**: 2258-2273. https://doi.org/10.1021/acs.langmuir.7b04076

[25] Ghosh S. Extraction of azo dye molecules from aqueous solution using polyamidoamine dendrimer based polymeric network. Journal of Chemical Research, 2008, 419-421. https://doi.org/10.3184/030823408785702481

[26] Parasuraman D and Serpe MJ. Poly (N-Isopropylacrylamide) Microgels for Organic Dye Removal from Water. ACS Applied Materials & Interfaces, 2011, **3**: 2732-2737. https://doi.org/10.1021/am2005288

[27] Ghosh S, Acharyya M, *et al*. Removal of Azo Dye Molecules from Aqueous Solution Using Novolac Resin Based Network Polymer. Bulletin of the Chemical Society of Japan, 2011, **84**: 349-351. https://doi.org/10.1246/bcsj.20100245

[28] Gao H, Kan T, Zhao S, *et al*. Removal of anionic azo dyes from aqueous solution by functional ionic liquid cross-linked polymer. Journal of Hazardous Materials, 2013, **261**: 83-90. https://doi.org/10.1016/j.jhazmat.2013.07.001

[29] Shalaeva YV, Morozova JE, Mironova DA, *et al*. Amidoamine calix[4]resorcinarene-based oligomers and polymers as efficient sorbents of azo dyes from water. Supramol. Chemical, 2015, **27**: 595-605. https://doi.org/10.1080/10610278.2015.1046455

[30] Yang D, Qiu L and Yang Y. Efficient Adsorption of Methyl Orange Using a Modified Chitosan Magnetic Composite Adsorbent. Journal of Chemical & Engineering Data, 2016,**61**: 3933-3940. https://doi.org/10.1021/acs.jced.6b00706

[31] Ghosh S and Acharyya M. Design of novolac resin-based network polymers for adsorptive removal of azo dye molecules. RSC Advances, 2016, **6**: 28781-28786. https://doi.org/10.1039/C6RA01903J

[32] Ghosh S, Acharyya M and Manna SC. Novolac Resin-Based Networks for Adsorptive Removal of Azo Dye (Orange-II) American Journal of Chemistry and Application, 2018, **5**: 29-34.

[33] Wang Y, Xie Y, Zhang Y, *et al*. Anionic and cationic dyes adsorption on porous poly-melamine-formaldehyde polymer. Chemical Engineering Research and Design, 2016, **114**: 258-267.
https://doi.org/10.1016/j.cherd.2016.08.027

[34] Kyzas GZ, Bikiaris DN and Mitropoulos AC. Chitosan adsorbents for dye removal: a review. Polymer International, 2017, **66**: 1800-1811.
https://doi.org/10.1002/pi.5467

[35] Li C P, Zhou H, Wang S, *et al*. A nanoporous Ag(I) coordination polymer for selective adsorption of carcinogenic dye Acid Red 26. Chemical Communication, 2017, **53**: 4767-4770.
https://doi.org/10.1039/C7CC02005H

[36] Singha NR, Karmakar M, Mahapatra M, *et al*. Systematic synthesis of pectin-g-(sodium acrylate-co-N-isopropylacrylamide) interpenetrating polymer network for superadsorption of dyes/M(II): determination of physicochemical changes in loaded hydrogels. Polymer Chemistry, 2017, **8**: 3211-3237.
https://doi.org/10.1039/C7PY00316A

[37] Fu D, Keech PG, Sun X, *et al*. Iron oxyhydroxide nanoparticles formed by forced hydrolysis: dependence of phase composition on solution concentration. Physical Chemistry Chemical Physics, 2011, **23**: 18523-18529.
https://doi.org/10.1039/c1cp20188c

[38] Mena-Duran CJ, Kou MRS, Lopez T, *et al*. Nitrate removal using natural clays modified by acid thermoactivation. Applied Surface Science, 2007, **253**: 5762-5766.
https://doi.org/10.1016/j.apsusc.2006.12.103

[39] Cundy AB, Hopkinson L and Whitby RLD. Use of iron-based technologies in contaminated land and groundwater remediation: A review. Science of the Total Environment, 2008, **400**(1-3): 42-51.
https://doi.org/10.1016/j.scitotenv.2008.07.002

[40] Freundlich HMF. Over the adsorption in solution. Journal of Physical Chemistry, 1906, **57**: 385-470.

[41] Foo KY and Hameed BH. Insights into the Modeling of Adsorption Isotherm Systems. Chemical Engineering Journal, 2010, **156**: 2-10.
https://doi.org/10.1016/j.cej.2009.09.013